

High throughput mechanobiology screening platform using micro- and nano-topography

Junqiang Hu^{†,§,‡}, Alexander A. Gondarenko^{†,§,‡}, Alex P. Dang[¶], Keenan T. Bashour^{§,¶}, Roddy S. O'Connor^{§,#}, Sunwoo Lee[¶], Anastasia Liapis^{§,Δ}, Saba Ghassemi^{§,#}, Michael C. Milone^{§,#}, Michael P. Sheetz^{§,▼}, Michael L. Dustin^{§,Δ}, Lance C. Kam^{§,¶}, James C. Hone^{†,§,*}

[†]Department of Mechanical Engineering, Columbia University, New York, NY, 10027

[§]The Nanomedicine Center for Mechanobiology, Columbia University, New York, 10027

[¶]Department of Biomedical Engineering, Columbia University, New York, NY, 10027

[#]Department of Pathology and Laboratory Medicine, Perelman School of Medicine, University of Pennsylvania, Philadelphia, PA, 19104

[¶]Department of Electrical Engineering, Columbia University, New York, NY, 10027

^ΔDepartment of Pathology, New York University School of Medicine, New York, NY, 10016

[▼]Department of Biological Sciences, Columbia University, New York, NY, 10027

[‡] These authors contributed equally to this work

* Corresponding author, jh2228@columbia.edu

ABSTRACT

We demonstrate the first 96-well plate platform to screen effects of micro- and nano-topographies on cell growth and proliferation. Existing high-throughput platforms test a limited number of factors, and are not fully compatible with multiple types of testing and assays. This platform is compatible with high throughput liquid handling, high-resolution imaging and all multiwell plate-based instrumentation. We use the platform to screen for topographies and drug-topography combinations that have short- and long-term effects on T-Cell activation and proliferation. We coated nanofabricated “trench-grid” surfaces with anti-CD3 and anti-CD28 antibodies to activate T-cells, and assayed for interleukin 2 (IL-2) cytokine production. IL-2 secretion was enhanced at 200 nm trench width and $>2.3 \mu\text{m}$ grating pitch; however, the secretion was suppressed at 100 nm width and $<0.5 \mu\text{m}$ pitch. The enhancement on 200 nm grid trench was further amplified with the addition of blebbistatin to reduce contractility. 200 nm grid pattern also showed great potential in T-cell long-term expansion and restimulation.

KEYWORDS: High throughput screening, nanotechnology, T-cell, Interleukin-2, Lck, Long-term expansion

TEXT

Surface topography can influence cell shape, expansion, proliferation, differentiation, and motility.¹⁻⁵ This topography can include three-dimensional structures such as gels⁶ and fibrous scaffolds,^{7,8} and two-dimensional surfaces patterned with features on the micro- and nanometer scale. Micro scale topographies such as gratings can influence the shape and motility of attached cells.⁹ Nano scale gratings also been used to study the differentiation and proliferation of human mesenchymal stem cells (hMSCs).¹⁰ Alternatively, limiting the adhesion area on flat substrates by microprinting proteins on flat substrates can shape the 2D geometry of attached cells.¹¹ Nano-scale cues can arise from clustering of integrins and other adhesion molecules to features in the extracellular matrix (ECM).¹²⁻¹⁴ Artificial ECMs to control integrin clustering have used fibrous materials, rough surfaces, micro topographies of adhesive islands and other parameters.^{7,8,11,15,16} Lymphocytes have surface features such as microvilli and ruffles that have nano-scale dimensions and may interface with nanofabricated features such as a surface trenches presented in a grating or grid pattern.

The complexity of cellular interactions with nano-topography has motivated development of high-throughput platforms in which many such patterns can be studied at once. Three such systems are summarized in table 1. The TopoChip system¹⁷ has 2176 nanotopographies on a single surface, and has been used to identify unique topographies able to affect human mesenchymal stromal cells proliferation and osteogenic differentiation. The BSSA system¹⁸ consists of a 3x3mm chip area consisting of 504 different microstructures, and has been used to study expansion and differentiation of embryonic stem cells. Optimal topography for directing

the differentiation of primary murine neural progenitor cells was identified by the customizable multi-architecture chip (MARC).¹⁹

Here we demonstrate an Integrated Mechanobiology Platform (IMP) that, like these systems, allows study of cell growth and proliferation on multiple nano-topographies. The IMP consists of standard, high-throughput well plate frame bonded with bottoms made from polydimethylsiloxane (PDMS) that present different surfaces in each compartment. Integration into the well-plate format is the distinctive aspect of the IMP, and allows for three important advantages relative to previous work. First, isolation of each pattern into a separate well allows testing of behaviors that can be affected by cross-contamination of soluble factors, such as cell proliferation and differentiation. Second, the well plate format allows for implementation of new assays, such as flow cytometry and ELISA, that require cell populations and supernatant that are separated into distinct wells. Third, the format allows for robotic liquid handling and high-throughput screening using the broad technology base developed around multi-well plates. As a final added advantage, the PDMS can be cast to the thickness of standard cover slips to allow high-resolution microscopy.

Table 1: Comparison of high throughput screening systems

	IMP	TopoChip	BSSA	MARC
Pattern format	Single or multiple pattern per well. 96, 384 well plate.	2176 patterns on 2cm×2cm area. Circles, isosceles triangles, thin rectangles	169 squares, each covers 3mm×3mm area	6x6 array of 18 patterns on 2.2cm×2.2cm
Transmission Microscopy	yes	yes	no	no
High NA Microscopy	yes	no	no	no

Form Factor	Tissue culture plate	Microarray chip	Microarray chip	Microarray chip
Automated Fluidic Handling	yes	no	no	no
Plate scanner readout	yes	no	no	no

Figure 1 shows the process to fabricate the IMP. First, we use electron-beam lithography and plasma etching to create a silicon mold. PDMS is then molded from this pattern in a jig that produces a controlled thickness. The PDMS is then bonded to a standard bottomless microplate through oxygen plasma and aminosilane-mediated treatment.²⁰ Irreversible bonding is formed in the interface of the PDMS and polystyrene (PS) thermoplastic under pressure. Here the system is demonstrated on 96-well plates, but has also been tested on 384-well plates and is easily extended to plates with smaller well size (up to 9600 wells).

We demonstrate the versatility of the IMP by assaying the effects of nano-scale topographies on activation and proliferation of human T-cells. T-Cells orchestrate adaptive immune response in the mammalian organisms. The response is initiated by interaction of a T-cell with an Antigen-Presenting Cell (APC).²¹⁻²⁴ Studies of the cell-cell interface have demonstrated that the micro- and nano-scale organization of signaling complexes between the APC and the T-Cell modulate the initial signaling including the interdigitated nanoscale projections and transfer of nanoscale vesicles.^{25,26} Development of a controllable platform for ex vivo activation of T-Cells is central to immunotherapy for treatment of variety of diseases, including cancer and chronic viral infections as well as basic studies of T-Cell signal transduction.^{27,28} In several adoptive immunotherapy strategies, populations of T-cells are isolated from the patient and expanded ex vivo in order to produce clinically effective numbers of cells and carry out manipulations including introduction

of genes needed for targeting; the resultant cellular product is then transfused back into the patient. The expansion process begins with cellular activation, most commonly with antibodies to the T cell antigen receptor (anti-CD3) and the costimulatory receptor CD28 (anti-CD28)²⁹, both attached to a rigid support. Previous studies have shown that altered substrate rigidity can further enhance T cell expansion in *ex vivo* cultures,³⁰ indicating that mechanical interaction with the substrate can affect the expansion process.

T-cell responses to antibody-coated substrates progresses in stages. Initially, the T-cell binds and spreads on the ACS.³¹ After several hours the cells detach while secreting IL-2 and other cytokines that act as paracrine growth and differentiation factors.³² The cells increase in volume and the first mitosis occurs within 3 days. They continue to undergo rapid mitosis for a week or longer depending on the exact culturing conditions.³⁰ Our platform enabled us to collect and correlate data through all three stages of cell culture. Specifically, we imaged cell morphology within 1-4 hours of exposure to expansion culture with fluorescent confocal microscopy; we also imaged fixed cells at high resolution using scanning electron microscopy (SEM). We identified early divisions within 3 days using flow cytometry and measured IL-2 secretion using ELISA.³³ Further, we performed flow cytometry over a period of 2 weeks to measure doublings and initiated by the substrates with varied topography. Finally, we repeated some of the experiments with addition of cytoskeleton inhibitors to analyze effects of topography-drug combinations on cell expansion. Dynal beads immobilized with anti-CD3/CD28 antibodies are currently the standard substrates for T cell expansion for immunotherapy applications.³⁴ Thus flat surfaces and dynal beads coated with anti-CD3/CD28 were applied in our experiments as controls to compare with the effects from micro- and nano-scale topographies.

Because T cell surfaces are covered with protrusions in the steady state which undergo remodeling during activation, we concentrated on topographies with trenches of variable nanoscale width and varying pitch in a simple grating and grid patterns, as shown in 2A and 2E. The gratings tested had a pitch of 3.0-0.3 μ m with 50% duty cycle, and the depth is 800 nm. The grids were composed of 300 nm deep trenches, 300-65 nm wide, in a square pattern with 750 nm pitch unless specified otherwise. Within one hour of attachment to these patterns, the cells spread over the ACS, after which they slowly contract and mostly detach after 4 hours. Therefore, we fixed and stained the cells for actin after 1,2,3, and 4 hours of culture, and quantified the shape of more than 1,000 cells by ImageJ. Cells cultured on gratings spread along the grating direction within the first hour, as the initial TCR engagement will lead to enhanced phosphorylation, larger contacts will lead to better activation. Actin polymerization and tyrosine kinase activation drive the protrusion formation along the gratings³⁵. When the cells are fully activated, there will be less activation of actin polymer, however, the myosin will exert a centripetal contraction force that maintains at certain level to keep synaptic integrity over time.^{36,37} Decreasing protrusion force of actin will make the contraction behavior by myosin become dominant. After initial spreading, the length and aspect ratios decreased as the cells contracted, Fig. 2D. The gratings also inhibited spreading perpendicular to the grating direction, SFig. 1A. Likewise, the alignment of the cell major axis to the grating was largest in the first hour and decreased as cells contracted, SFig. 1B. Cells on grids demonstrated reduced spreading area as the trench width decreased, Fig. 2K. Confocal and SEM imaging revealed that the cell spreading is arrested at the narrowest trenches, Fig. 2F-J. Whereas the T-Cells were able to spread by protruding into the wider trenches, the leading edge of the cell is apparently not able to protrude into the narrowest trenches, nor to ‘hop’ over them. As we know, the interaction of T-cells with its external

physical environment will have effects on cell signaling and cell fate. We will demonstrate what the physical impacts are in terms of T cell activation, expansion and interleukin secretion.

Here we demonstrated that different spreading patterns on the nano-topographies led to different levels of T-cell proliferation and activation as indicated by secretion of cytokines such as IL-2 and expansion index. IMP system enables the high-throughput examination of IL-2 secretion. Proliferation and IL-2 secretion were measured after 2 days by fluorescence-activated cell sorting (FACS) and ELISA, respectively. Proliferation is measured based on expansion index, which measures the fold-expansion of the overall culture. For example, expansion index of 2 means the total cell count is doubled after a certain period of culturing. IL-2 concentration was analyzed by Multiskan FC (Thermo Scientific) plate reader with two readings from 450 nm and 540 nm filters.

The IMP allows easy testing of multiple samples due to the well plate format. This allows us to examine the variability due to the use of multiple donors in human T-cell experiments. IL-2 baseline secretion may vary from donor to donor due to factors such as genetics, age, gender and if the donor was sick or healthy. The heat map of IL-2 secretion in Fig. 3B shows IL-2 levels from T-cells from 4 different donors, tested on 4 different grid geometries, with 6 replicates for each combination. IL-2 secretion was normalized to each donor baseline secretion and we observed that the fold change of IL-2 secretion for each donor is consistent across different donors due to different grid geometry they exposed to.

For grid geometries, we tested a wide range of grid geometry parameters to separate the effects of trench width, trench pitch, and area of the pedestal isolated by the trench, SFig. 2A. Briefly, the trench width was found to be the most significant variable modifying secretion of IL-2, with

significant inhibition for 100 nm trench widths. However, even 100 nm trenches spaced significantly far apart no longer inhibited IL-2 secretion, SFig. 2B. IL-2 secretion levels for 750 nm pitch grids with 100, 200, and 300 nm trenches, as well as flat substrates, are shown in Fig. 3A; the 100 nm trenches show a 2-fold decrease in IL-2 secretion compared to the flat substrate, while 200 nm trenches showed a 30% increase. Grating geometries demonstrated similar trends: IL-2 secretion was higher for longer grating pitches, and for short pitches, there is an obvious IL-2 secretion inhibition, Fig. 3C. Cell proliferation, as measured by the expansion index, is shown for each pattern in Figs. 3A and 3C. For grids with 100 nm trenches, inhibition of IL-2 secretion also strongly correlated with decreased cell proliferation, but no increase in proliferation is seen for 200 nm trenches. Surprisingly, the opposite pattern is seen for gratings: proliferation increases for narrower pitches while IL-2 decreases.

These results strongly suggest that physical interaction with different grid patterns directly affects the signaling leading to T-cell activation. Because TCR signaling begins with phosphorylation of the CD3 complex units containing immunoreceptor tyrosine-based activation motifs (ITAMs) by the Src family tyrosine kinase Lck,^{38,39} we imaged Lck microclusters (MCs) on grids after 1 hour of activation (Fig. 3D). Compared to flat substrates, 300 nm grids show similar MCs density, 200 nm grids show an increase, and 100 nm grids show the lowest density. This is confirmed by statistical analysis of Lck MCs size versus the total cell size, Fig. 3E. The trend in MC formation directly follows IL-2 secretion (Fig. 3A), indicating that the IL-2 secretion variance on grids can be tracked back to early stage cell signaling. It has been shown that Lck phosphorylation activity is suppressed by the presence of tyrosine phosphatases such as CD45, which dephosphorylate ITAMs.⁴⁰ Thus the exclusion of CD45 will thus favor stronger T-cell activation. We postulate that 100 nm grid pattern interacts with the T-cell to create a channel

for the entry of CD45 to the TCR engagement sites, resulting in less Lck MCs and suppressed IL-secretion. However, the details of this process are still unknown and motivate further study.

Another distinguishing advantage of IMP is that the well-plate format makes long-term culture straightforward for study of proliferation over many days. In this study, mixed CD4⁺ / CD8⁺ cells were isolated from whole blood from healthy patients and were seeded at 10⁶ / mL (200 k cells in 200 μ L) (37 °C, 5% CO₂). Cell proliferation was assessed beginning on day 3 post-seeding and every other subsequent day. The proliferation index was determined via carboxyfluorescein succinimidyl ester (CFSE) staining on day 3 post-seeding with flow cytometry. Cells were frozen down for restimulation (to mimic the adoptive immunotherapy process) on completion of the blasting phase. In Fig. 4A, two groups of experiments were carried out either with or without addition of IL-2 (50ng/ml) at the beginning of culture to enhance the activation. Without added IL-2, cell population reached a maximum at around day 13, and 100- and 200 nm grid patterns outperformed Dynal beads. With added IL-2, expansion increases obviously on 100 nm patterns. This is understandable given the fact that 100 nm grids show the lowest IL-2 secretion at day 3 (Fig. 3). The largest difference of the cell doubling between patterns and Dynal beads is ~1.5 doublings (i.e. a nearly 3-fold increase in expansion). Moreover, the expansion speed is much faster: expansion on Dynal beads reaches a maximum at day 11, whereas the 200 nm grids yield the same level 2 days earlier (at day 9). The functionality of these cells is evaluated by the IFN- γ expression percentage. Fig. 4B shows that cells stimulated on grids and Dynal beads show a similar IFN- γ expression, confirming that expansion on grids provides the observed expansion enhancement with no apparent loss of functionality.

The microplate format of IMP also allows straightforward study of the combined effects of drugs and topography, to determine whether chemical factors can interact with geometric cues and

affect cell activation metrics. Actin polymerization and myosin contractions are believed to play a central role in actomyosin retrograde flow, MCs centralization and sustained Ca^{2+} signaling, which are critical for T-cell signaling and activation.³⁷ Therefore we screened several cytoskeleton inhibitors (Latrunculin B, Jasplakinolide, and Blebbistatin) in combination with grid geometries. Latrunculin B (LatB) is an F-actin depolymerizing agent inhibiting formation of microcluster.³⁵ Jasplakinolide (Jasp) is an F-actin stabilizing agent that perturbs actin turnover.⁴¹ Blebbistatin (Blebb) is a inhibitor of myosin II ATPase activity.⁴² All inhibitors were added 5 minutes post cell-seeding. Fig. 5A shows that IL-2 secretion on grids is comparable for controls and LatB treated cells, and strongly suppressed for Jasp. Surprisingly, we found strong drug/geometry interaction in T-cells cultured on grids and exposed to blebbistatin. The general trend follows the one from IL-2 study of Fig. 3C; however, the enhancement or inhibition of the IL-2 secretion was amplified with the addition of blebbistatin. In particular, we observed a 162% enhancement in IL-2 secretion after 2-3 days of culture (Fig. 5B). The lack of an effect due to Lat B is explained by the rapid (< 5 min.) assembly of microclusters:³⁷ although LatB inhibits the formation of new MCs by actin depolymerization, existing MCs are stable. On the other hand, Jasp perturbs actin turnover, freezing the actin networks, and causing the loss of phosphor-PLC γ 1 in T-cell activation, and further shutting down Ca^{2+} signaling. The detailed mechanism for the geometry-dependent effects of Blebbistatin is still unknown; however, we postulate that the loss of myosin contraction enhances the effect of segregation of CD45 on 200 nm grids and the entry of CD45 on 100 nm grid.

In conclusion, we have demonstrated an Integrated Mechanobiology Platform to study cellular interactions with nano-topographies. The IMP system uses a standard well plate format, and is compatible with existing high throughput technologies such as plate readers, multi channel

pipettes, and fluidic handling robots. And these enable us to incorporate new high throughput assays such as ELISA, long-term expansion and drug-topography effects. As a demonstration, the IMP was used to screen the effects of nano-topographies on activation of T-Cells. In a study of 100s of samples over a dozen geometries, we discovered significant changes in T-Cell activation response in grids with gaps from 300 nm to 100 nm. In particular, the 200 nm grid pattern provided a 3-fold increase in expansion with no change in functionality. These findings confirm that cell expansion and restimulation can be strongly modified by early stage physical interaction with the substrate topography, as confirmed by imaging of MC formation and drug inhibition studies. They further motivate future research into the details of the geometric interaction, for instance to measure and understand CD45 segregation on grid patterns. The IMP format directly facilitates these findings by allowing efficient exploration of multiple geometries in separate wells for independent long-term culture, combined with compatibility with multiple assays of cell behavior.

FIGURES

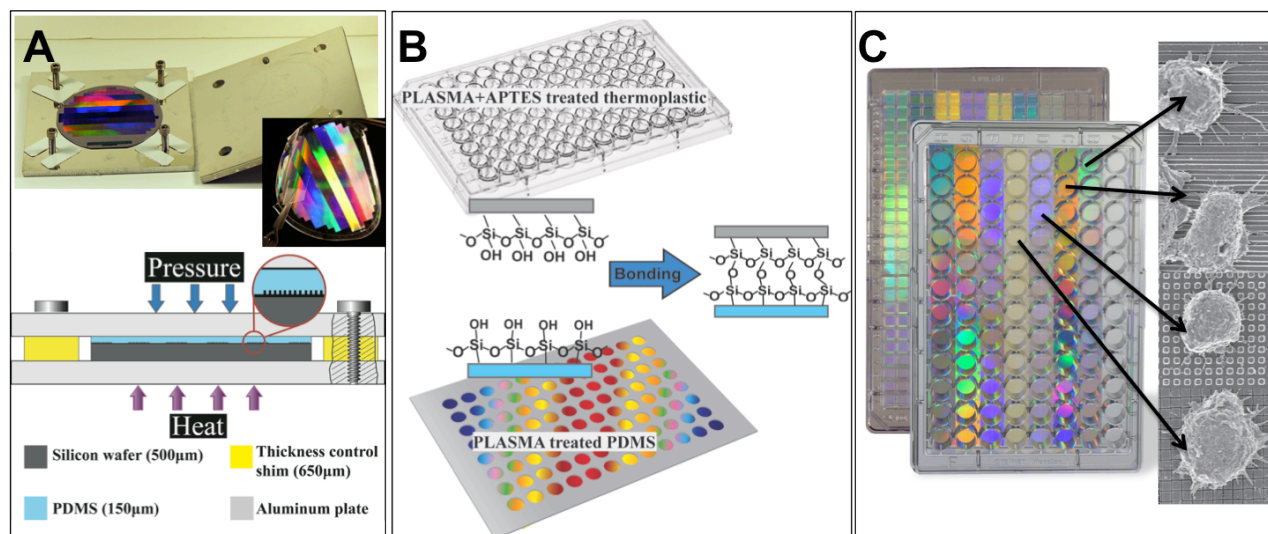


Figure 1. IMP fabrication process. A. Bonded plates assembly, PDMS thickness is controlled by changing the relative thickness of Si wafer and the shims in four corners, PDMS sheet thickness is ~150 μm; B. thermoplastic plate is first O₂ plasma treated for 1 minute and then treated with 1.5% of APTES solution for 20 minutes, patterned PDMS substrate is O₂ plasma treated for 1 minute, a silane coupling reaction followed by amine-epoxy bond formation at the interfaces of treated thermoplastic and PDMS at room temperature; C. Integrated Mechanobiology Platform, in a 96 well plate configuration. The bottom surface of the plate is composed of PDMS nanopatterns.

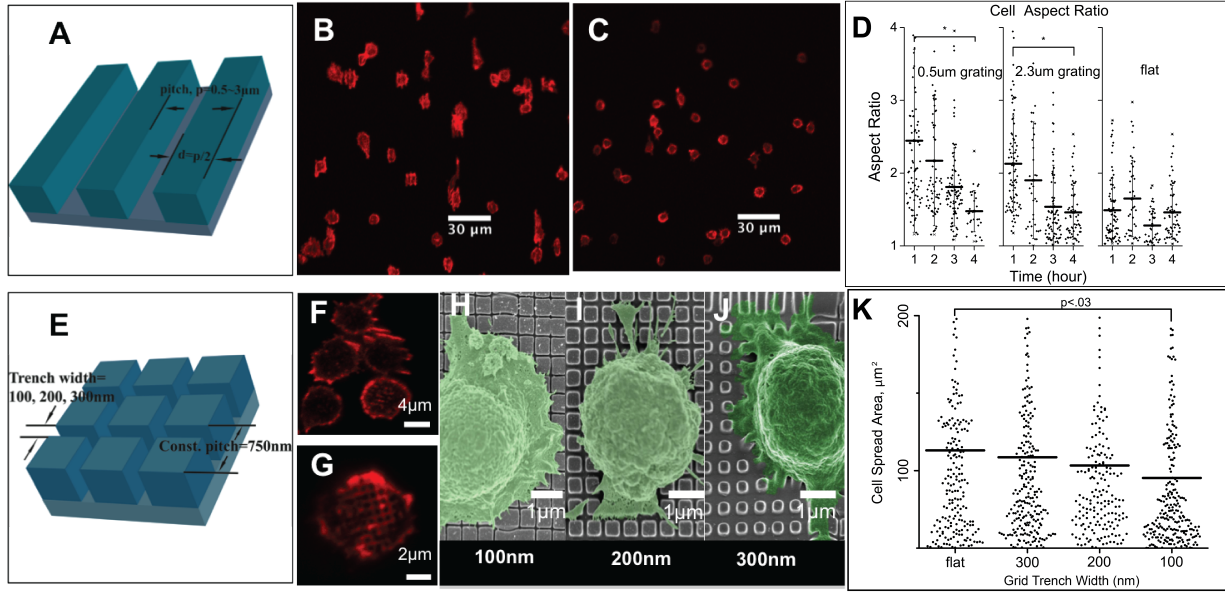


Figure 2. IMP compatibility with various imaging microscopy. A. 3D perspective of grating geometry; 50% duty cycle and the pitch varies from 500 nm to 3000 nm; B. The cells spread along the direction of the grating (vertical) within the first hour; C. The cells stop spreading and start contracting after 4 hours; D. Aspect ratio of T-Cells activated on grating and flat PDMS; E. 3D perspective of grid, grid geometry is a square lattice of trenches on a 750 nm pitch, trench width is 100-300 nm; F-G. High-resolution confocal imaging of actin in T-Cells on 100 nm and 300 nm grid geometries; H-J. High-resolution imaging of colorized Scanning Electron Micrograph (SEM) of T-Cells on grid geometries; K. T-Cell spreading area on grid geometries.

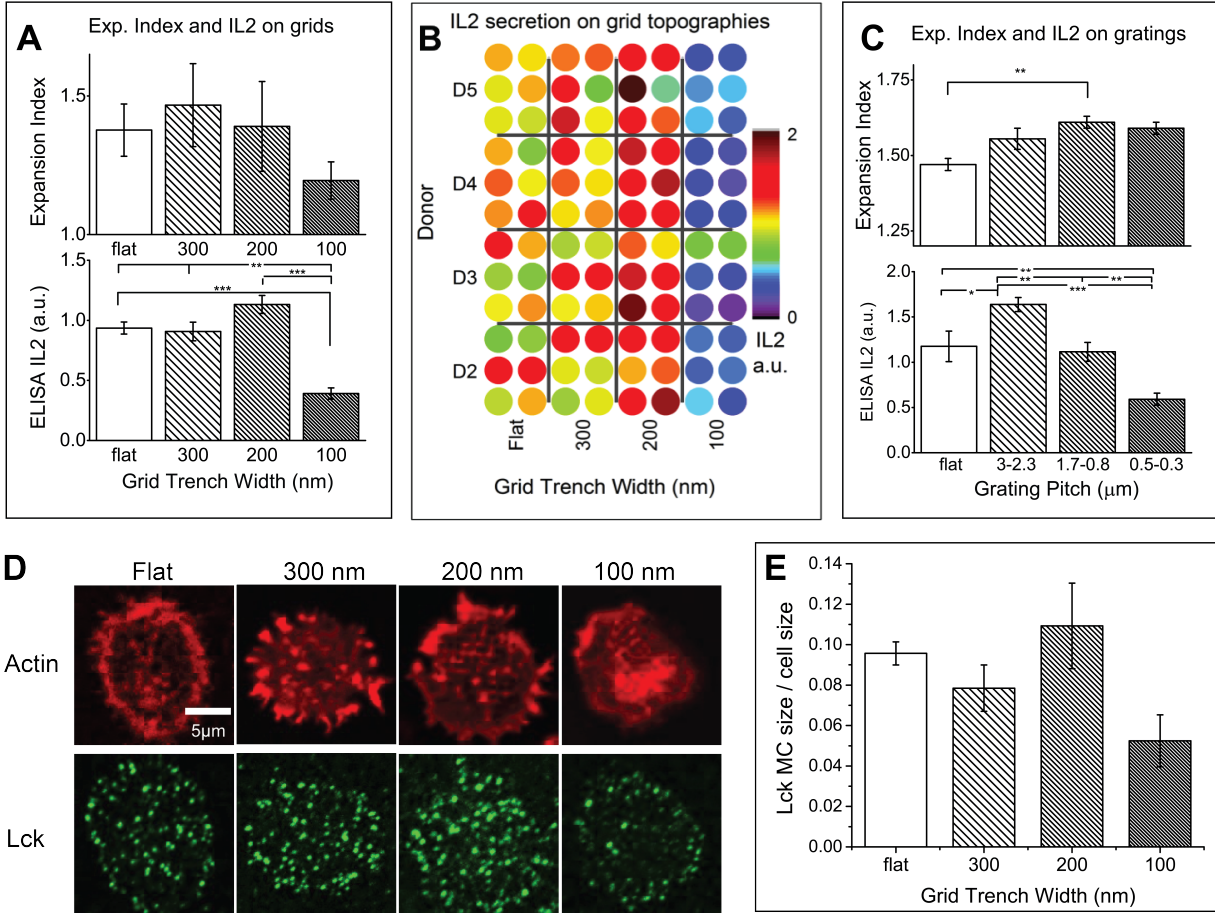


Figure 3. IMP compatibility with plate readers. A. Expansion Index and supernatant IL-2 from T-Cells activated on grating geometries; B. ELISA IL-2 measurements from a well plate with 96 samples of 4 donors and 4 different topographies tested; C. Expansion Index and supernatant IL-2 from T-Cells activated on grid topographies after 2-3 days culturing; D. Actin and Lck microcluster staining after 1 hour culture on grid patterns; E. Statistical analysis of Lck microcluster size versus total cell size, and the percentage trend correlates with IL-2 secretion shown in Fig. 3A. (*, $p < 0.01$; **, $p < 0.005$; ***, $p < 0.00005$)

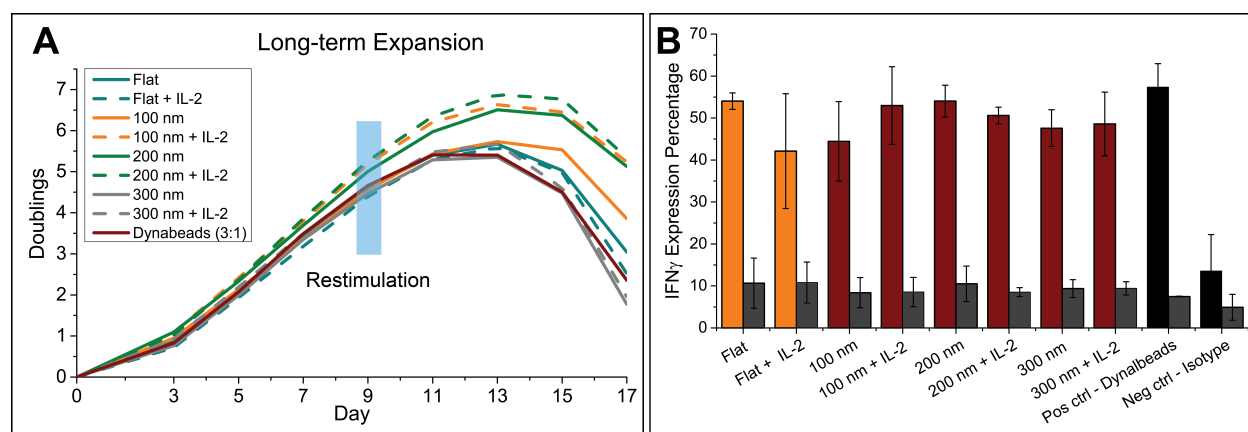


Figure 4. T-cell long-term expansion and restimulation on grid patterns. A. Two groups experiments carried out, one without additional IL-2 and the other group with 50ng/ml IL-2 addition at the beginning of cell culture. Cell induction and proliferation were assayed by CFSE dilution every two days from day 3 and at day 9 cells were frozen down for restimulation; B. Cells were restimulated by Dynal beads and IFN- γ expression percentage is analyzed for the study of cell functionality, grid patterns showed less but comparable percent of IFN- γ comparing with Dynal beads.

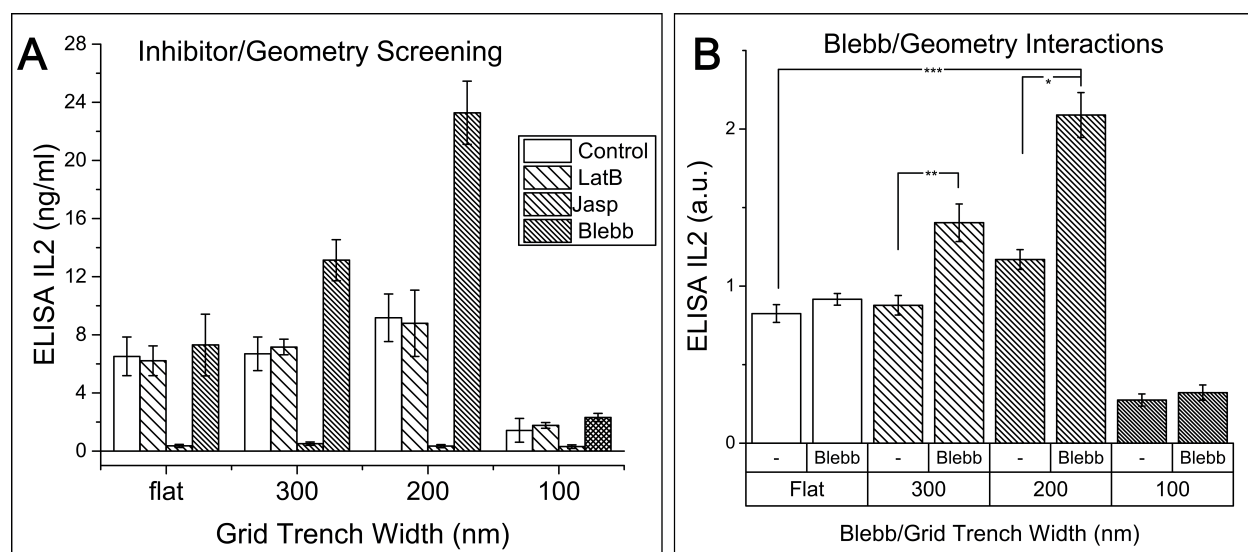


Figure 5. IMP compatibility for study of topography-drug combinations on cell expansion. A. Three inhibitors (Latrunculin B, Jasplakinolide and Blebbistatin) were tested for a drug/geometry combination effects on cell behavior. There is a drug/geometry interaction with 200 nm grids and blebbistatin; B. IL-2 secreted in supernatant after 2-3 days of culture on grid geometriess with and without Blebbistatin. Two-way repeated measure ANOVA analysis shows significant enhancement in IL-2 secretion with Blebbistatin & 200 nm trench geometry combination. (*, $p<0.02$; **, $p<0.3$; ***, $p<0.0002$)

ASSOCIATED CONTENT

Supporting Information. Information on IMP fabrication, cell preparation and analysis, along with details on the experimental measurements and methods, and supplementary Figure 1-4. This material is available free of charge via the Internet at <http://pubs.acs.org>

AUTHOR INFORMATION

Corresponding Author

*Email: jh2228@columbia.edu

Author Contributions

‡These authors contributed equally.

J.H., A.A.G., and A.P.D. designed the experiments. J.H., A.A.G. and A.P.D. carried out fabrication, performed the experiments and analyzed data, and S.L. assisted with the fabrication. L.C.K., K.T.B., R.S.O., S.G., A.L., M.C.M., M.P.S. and M.L.D. provided assistance with data interpretation. J.H., A.A.G. and J.C.H. wrote the paper. L.C.K. and M.L.D. helped with revising the paper. All authors discussed the results and commented on the manuscript.

Notes

The authors declare no competing financial interest.

ACKNOWLEDGMENT

This work was supported by National Institutes of Health (PN2EY016586). As members of the Nanomedicine Center for Mechanobiology, we thank all the researchers in the center for the discussion of this work. We also thank Professor Lance C. Kam for providing lab space and consumables at the beginning of this project. We thank Geraldine Goebrecht for assistance with flow cytometry. In addition, we thank Dr. Joung-Hyun Lee from Prof. Lance C. Kam's lab for the discussion on data presented in the paper.

REFERENCES

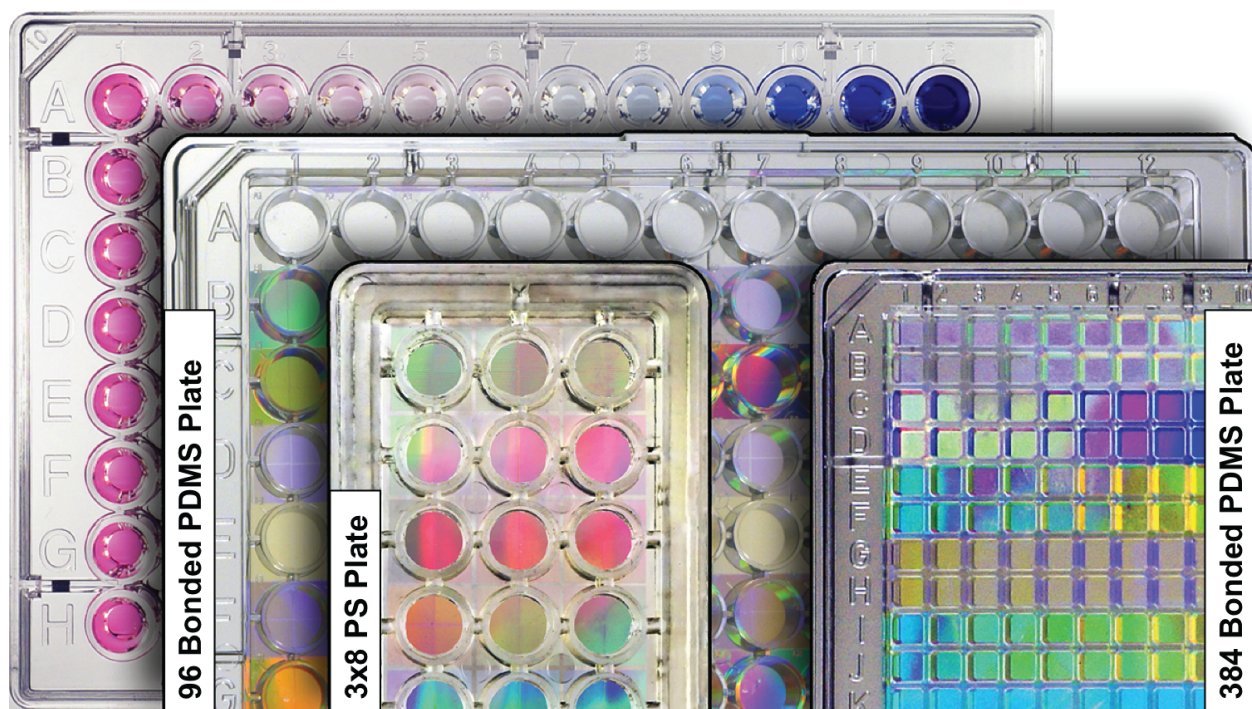
1. Chen, C. S. Geometric Control of Cell Life and Death. *Science* 276, 1425–1428 (1997).
2. Juliano, R. L. & Haskill, S. Signal transduction from the extracellular matrix. *J. Cell Biol.* 120, 577–585 (1993).
3. Flemming, R. G., Murphy, C. J., Abrams, G. A., Goodman, S. L. & Nealey, P. F. Effects of synthetic micro-and nano-structured surfaces on cell behavior. *Biomaterials* 20, 573–588 (1999).
4. Bettinger, C. J., Langer, R. & Borenstein, J. T. Engineering Substrate Topography at the Micro- and Nanoscale to Control Cell Function. *Angew. Chem. Int. Ed.* 48, 5406–5415 (2009).
5. Anselme, K. et al. The interaction of cells and bacteria with surfaces structured at the nanometre scale. *Acta Biomater.* 6, 3824–3846 (2010).
6. Tibbitt, M. W. & Anseth, K. S. Hydrogels as extracellular matrix mimics for 3D cell culture. *Biotechnol. Bioeng.* 103, 655–663 (2009).
7. Freed, L. E. et al. Biodegradable Polymer Scaffolds for Tissue Engineering. *Nat. Biotechnol.* 12, 689–693 (1994).
8. Lee, J., Cuddihy, M. J. & Kotov, N. A. Three-Dimensional Cell Culture Matrices: State of the Art. *Tissue Eng. Part B Rev.* 14, 61–86 (2008).
9. Yim, E. et al. Nanopattern-induced changes in morphology and motility of smooth muscle cells. *Biomaterials* 26, 5405–5413 (2005).

10. Yim, E. K. F., Pang, S. W. & Leong, K. W. Synthetic nanostructures inducing differentiation of human mesenchymal stem cells into neuronal lineage. *Exp. Cell Res.* 313, 1820–1829 (2007).
11. Singhvi, R. et al. Engineering cell shape and function. *Science* 264, 696–698 (1994).
12. Werb, Z. ECM and cell surface proteolysis: regulating cellular ecology. *Cell* 91, 439–442 (1997).
13. Mark, K. von der, Park, J., Bauer, S. & Schmuki, P. Nanoscale engineering of biomimetic surfaces: cues from the extracellular matrix. *Cell Tissue Res.* 339, 131–153 (2010).
14. Shen, K., Milone, M. C., Dustin, M. L. & Kam, L. C. Nanoengineering of Immune Cell Function. in *MRS Proceedings* 1209, 1209–YY03 (Cambridge Univ Press, 2009).
15. Dalby, M. J. et al. The control of human mesenchymal cell differentiation using nanoscale symmetry and disorder. *Nat. Mater.* 6, 997–1003 (2007).
16. Reynolds, P. M., Pedersen, R. H., Riehle, M. O. & Gadegaard, N. A Dual Gradient Assay for the Parametric Analysis of Cell-Surface Interactions. *Small* 8, 2541–2547 (2012).
17. Unadkat, H. V. et al. An algorithm-based topographical biomaterials library to instruct cell fate. *Proc. Natl. Acad. Sci.* 108, 16565–16570 (2011).
18. Markert, L. D. et al. Identification of Distinct Topographical Surface Microstructures Favoring Either Undifferentiated Expansion or Differentiation of Murine Embryonic Stem Cells. *Stem Cells Dev.* 18, 1331–1342 (2009).
19. Moe, A. A. K. et al. Microarray with Micro- and Nano-topographies Enables Identification of the Optimal Topography for Directing the Differentiation of Primary Murine Neural Progenitor Cells. *Small* 8, 3050–3061 (2012).

20. Sunkara, V. & Cho, Y.-K. Investigation on the Mechanism of Aminosilane-Mediated Bonding of Thermoplastics and Poly(dimethylsiloxane). *ACS Appl. Mater. Interfaces* 4, 6537–6544 (2012).
21. Smith-Garvin, J. E., Koretzky, G. A. & Jordan, M. S. T Cell Activation. *Annu. Rev. Immunol.* 27, 591–619 (2009).
22. Bashour, K. T. et al. CD28 and CD3 have complementary roles in T-cell traction forces. *Proc. Natl. Acad. Sci.* 111, 2241–2246 (2014).
23. Bashour, K. T. et al. Cross Talk between CD3 and CD28 Is Spatially Modulated by Protein Lateral Mobility. *Mol. Cell. Biol.* 34, 955–964 (2014).
24. Deeg, J. et al. T Cell Activation is Determined by the Number of Presented Antigens. *Nano Lett.* 13, 5619–5626 (2013).
25. Biggs, M. J. P., Richards, R. G. & Dalby, M. J. Nanotopographical modification: a regulator of cellular function through focal adhesions. *Nanomedicine Nanotechnol. Biol. Med.* 6, 619–633 (2010).
26. Choudhuri, K. et al. Polarized release of T-cell-receptor-enriched microvesicles at the immunological synapse. *Nature* 507, 118–123 (2014).
27. Dustin, M. L. & Depoil, D. New insights into the T cell synapse from single molecule techniques. *Nat. Rev. Immunol.* 11, 672–684 (2011).
28. Maus, M. V. et al. Ex vivo expansion of polyclonal and antigen-specific cytotoxic T lymphocytes by artificial APCs expressing ligands for the T-cell receptor, CD28 and 4-1BB. *Nat. Biotechnol.* 20, 143–148 (2002).
29. Levine, B. L. et al. Effects of CD28 costimulation on long-term proliferation of CD4+ T cells in the absence of exogenous feeder cells. *J. Immunol.* 159, 5921–5930 (1997).

30. O'Connor, R. S. et al. Substrate Rigidity Regulates Human T Cell Activation and Proliferation. *J. Immunol.* 189, 1330–1339 (2012).
31. Yu, L. et al. Flow-through functionalized PDMS microfluidic channels with dextran derivative for ELISAs. *Lab. Chip* 9, 1243 (2009).
32. Shen, K., Thomas, V. K., Dustin, M. L. & Kam, L. C. Micropatterning of costimulatory ligands enhances CD4⁺ T cell function. *Proc. Natl. Acad. Sci.* 105, 7791–7796 (2008).
33. Dong, H., Zhu, G., Tamada, K. & Chen, L. B7-H1, a third member of the B7 family, co-stimulates T-cell proliferation and interleukin-10 secretion. *Nat. Med.* 5, 1365–1369 (1999).
34. Trickett, A. & Kwan, Y. L. T cell stimulation and expansion using anti-CD3/CD28 beads. *J. Immunol. Methods* 275, 251–255 (2003).
35. Bunnell, S. C., Kapoor, V., Triple, R. P., Zhang, W. & Samelson, L. E. Dynamic actin polymerization drives T cell receptor-induced spreading: a role for the signal transduction adaptor LAT. *Immunity* 14, 315–329 (2001).
36. Kumari, S. & Dustin, M. L. Immunology: Dendritic Cells Pull the T Cell's Strings. *Curr. Biol.* 25, R413–R415 (2015).
37. Babich, A. et al. F-actin polymerization and retrograde flow drive sustained PLC γ 1 signaling during T cell activation. *J. Cell Biol.* 197, 775–787 (2012).
38. Weiss, A. & Littman, D.R. Signal Transduction by Lymphocyte Antigen Receptors. *Cell* 76, 263–274 (1994).
39. Palacios, E. H. & Weiss, A. Function of the Src-family kinases, Lck and Fyn, in T-cell development and activation. *Oncogene* 23, 7990–8000 (2004).
40. Nika, K. et al. Constitutively Active Lck Kinase in T Cells Drives Antigen Receptor Signal Transduction. *Immunity* 32, 766–777 (2010).

41. Rubb, M.R. et al. Jasplakinolide, a Cytotoxic Natural Product, Induces Actin Polymerization and Competitively Inhibits the Binding of Phalloidin to F-actin. *J. Biological Chemistry* 269, 14869-14871 (1994).
42. Straight, A.F. et al. Dissecting Temporal and Spatial Control of Cytokinesis with a Myosin II Inhibitor. *Science* 299, 1743-1747 (2003).



For table of contents only